IDENTIFICATION OF BIOLOGICAL AND ANOMALOUS PROPAGATION ECHOES IN WEATHER RADAR OBSERVATIONS – AN IMAGING PROCESSING APPROACH

P11.123

Lin Tang*[1], Jian Zhang[1, 2], Yadong Wang[1], and Kenneth W. Howard[1, 2]

[1]Cooperative Institute for Mesoscale Meteorological Studies,
University of Oklahoma, Norman, OK, U. S. A.

[2]Natioanl Severe Storms Laboratory, Norman, OK, U.S.A.

1. INTRODUCTION

Radar echoes from migrating birds are usually considered as "contaminations" by weather radar users although the application of radars in bird identification is important for bird migration research (Schmaljohann et al., 2007) and studies of population dynamics of breeding seabird (HAMER et al., 2005) and roosting land birds (Bäckmanf and Alerstam, 2002). These contaminations in Doppler radar velocity (LIU et al., 2005; ZHANG et al., 2005) and reflectivity measurements (FULTON et al., 1998) are especially severe in the nighttime during migrating seasons. Radar echoes from migratory birds and moving insects often appear in expanding circular shapes on the reflectivity maps; therefore, they are usually referred as "bloom". Besides the bird migration in spring/fall seasons and nocturnal insects movement, another source of non-precipitation echoes is a type of ground clutter caused by the wave anomalous propagation (AP) (Martin and Shapiro, 2007). The air temperature usually decreases with height in the troposphere, but some times strong nocturnal radiation cooling at the surface can cause rapid decrease of temperature near the ground while the air aloft remains relatively warm. The strong vertical temperature inversion in the lower troposphere leads to the propagation of the electromagnetic (EM) wave bends toward the ground, which causes part of the radar beam hitting the ground and results in ground clutter contaminations in radar data.

Besides of the biological bloom echoes (insects, birds, bats, etc.) (Lakshmanan and Zhang, 2009) and AP (Moszkowicz et al., 1994; STEINER and SMITH, 2002), non-meteorological contamination of weather radar reflectivity data also includes the consistent ground clutter (Bachmann and Tracy, 2009), sea clutter (Gray and Larsen, 2004), chaff (metal strips) dropped by military aircraft, and etc.. Among these different types of clutter, bloom returns and AP are especially problematic due to their large areas and high intensities, particularly the magnitude, depth, and local texture of bloom are similar to widespread, shallow stratiform rains or snow (Lakshmanan et al., 2010). The movement of birds/insects crowd induces non-zero Doppler velocities (GAUTHREAUX and BELSER, 1998), making them difficult to be identified with zero-velocity criteria. (Lakshmanan et al., 2010) developed a technique to censor biological echoes with a neural network trained on historical cases. The real-time assessment in the United States indicates its capability of identifying and removing a good number of bloom echoes due to biological targets. However the technique shows limitation when various distributions of birds and their movements cause the bloom shape losing its symmetry. Further, this technique could not remove the bloom echoes when precipitation echoes exist within the same radar domain, even if the two types of echoes are isolated from each other.

A challenge for the quality control (QC) of AP echoes exists because the intensity and texture of AP returns are similar to those of strong and isolated convective cells. There have been many efforts (CHO et al., 2006; Pamment and Conway, 1998) trying to address the AP problems with different levels of success. In recent years, the quality control of weather radar data was improved with the help of other meteorological observations such as satellite images (Bøvith et al., 2006) and the multisource IR temperatures (Michelson and Sunhede, 2004). Nevertheless, AP and bloom contaminations remain a severe issue for radar precipitation estimation and operational hydrological applications. The National Weather Service (NWS) River Forecast Centers (RFCs) still devote significant resources to manually editing radar data and removing AP and bloom echoes from radar precipitation data. Therefore, an improved and automated radar quality control would be valuable to the NWS's hydrological operations.

The current study is a follow up to Lakshmanan et al. (2010) work, with a focus on further cleaning up AP and bloom echoes from based level radar reflectivity data in real-time. A new scheme was developed based on digital imaging processing techniques and large-scale physical characteristics of AP and blooms. Instead of local pixel analyses

*Corresponding author address: Lin Tang, Cooperative Institute for Mesoscale Meteorological Studies, University of Oklahoma, Norman, Oklahoma 73072; e-mail: lin.tang@noaa.gov

(Kessinger et al., 2003), reflectivity maps from different elevation angles and morphological characteristics of the base reflectivity images are treated globally. The methodology is described in the next section.

2. METHOD

In the study of Lakshmanan et al. (Lakshmanan et al., 2010), bloom echoes were assumed to be generally centered around the radar with a circularly symmetric shape. Based on this feature, a global mean reflectivity profile was used to distinguish blooms from precipitating echoes and all pixels were assigned a bloom probability for creating a local feature field. However, distributions of migrating birds and other biological objects are not always symmetric around the radar. As shown in Fig.1, the extent of non-symmetric bloom echoes varies from radial to radial. The symmetric characteristic of the bloom becomes weak and the bloom probabilities of the pixels are assigned low in these cases. As a result, blooms were retained leading to false estimation of light rain (< 35 dBZ) where there was no precipitation. The current study presents an approach that identifies blooms and AP echoes based on their global reflectivity features without a dependency on the symmetric property.

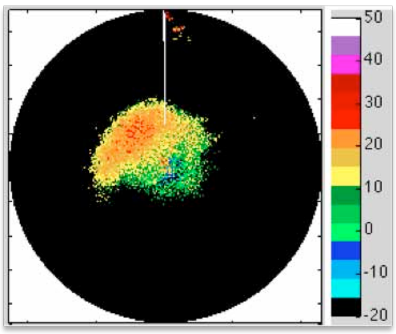

Figure 1. Bloom clutter without circular symmetry property (data from KHGX on May 10th, 2010 at 04:14 UTC).

(*a) Tilt Test*

One common characteristic of bloom and AP is the rapid decrease of echo areas from lower to upper tilts. This is a combined effect of vertical distributions of biological objects and the radar sampling geometry. The density of biological scatterers decreases with height and the maximum height that they can reach is usually below 3 km above mean sea level (Martin and Shapiro, 2007). Radar reflectivity observations are obtained on conical planes (or "tilts") with small positive elevation angles (Fig.2). Most of birds/insects' movement concentrates within the height of the lowest tilt, especially at medium to far ranges, resulting in a significantly larger echo area on the lowest tilt (e.g., e1 in Fig.2) than on the upper ones (e.g., e2 in Fig.2). Note that blooms may appear at higher altitude than they actually locate when nocturnal anomalous propagation combines with biological echoes. Similar feature is found in AP echoes where the strong power returns from the ground are confined in the lowest tilt and lack of vertical discontinuities. In the operational NWS radar Precipitation Processing System (FULTON et al., 1998), this feature was the basis for a so-called "tilt test" that reduced AP echoes in precipitation estimates. The same concept is extended in this study for identification of both AP and blooms.

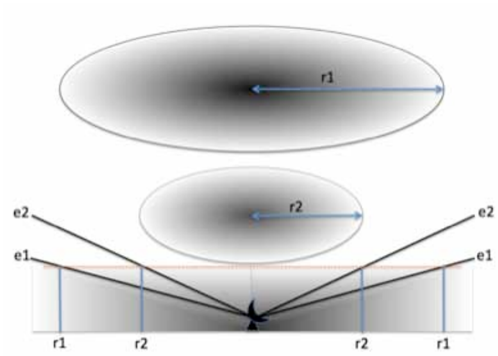

Figure 2. Illustration of biological scatterers distribution and the associated bloom echo distributions on the radar tilts. The grey shade represents the population density of birds/insects.

Fig. 3 shows the ratio of echo sizes between the 2nd and the 1st tilts for over 200 cases of pure bloom, AP, and precipitation echoes. The precipitation events included convective and stratiform rain as well as light and heavy snows. The echo size was defined as the number of pixels with reflectivity greater than a given threshold. Most severe AP echoes concentrate in the first peak bar at about 0.2-0.3 of size ratio (Fig. 3), indicating that strong AP from the ground has a more rapid size reduction in the vertical direction than blooms. Further, there is a general separation of ratio values between the non-precipitation and precipitation events, but with some overlapping between 0.5 and 0.7. The results indicates that the tilt test can be used as an effective pre-processing step to screen out many AP and bloom echoes, while further steps are required to separate non-precipitation and precipitation echoes for cases in the overlapping portion in Fig.3 and for cases with a mixture of clutter and precipitation echoes.

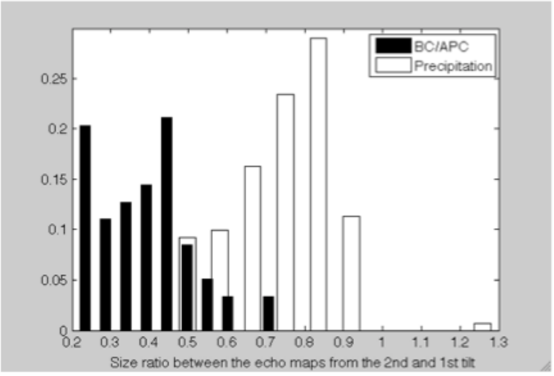

Figure 3. The size ratio between the echo maps from the 2nd and 1st tilt for BC/APC and precipitation weather conditions.

(*b) Entity Test*

The second characteristic of a bloom echo is the relative singularity of high reflectivity area, which generally concentrates at the center of the bloom with either a symmetrical or an asymmetrical shape. This is because a flock of migrating birds or moving insects usually has a maximum population in the center of the crowd and the population decreases outwards. Reflectivity echoes from a convective storm often show multiple high reflectivity entities associated with individual convective storm cells (Fig.4). Therefore an “entity test” is developed to identify blooms from convective precipitation.

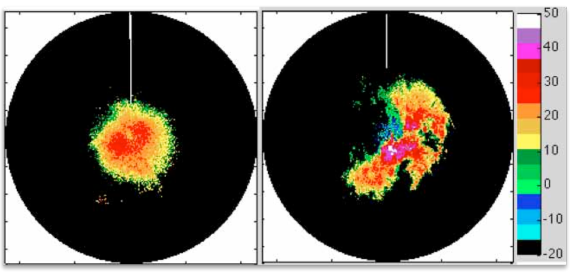

(a) (b)

Figure 4. Base reflectivity and echo entity map for a bloom event (a) and a convective storm event (b). Data are recorded from KFDR on May 7th, 2010 at 04:14 UTC (a) and KGGW on May 4th, 2010 at 04:52 UTC (b).

The entity test is applied to a reflectivity map on a given tilt and it consists of three steps: 1) filter out weak reflectivity echoes (i.e., the returns below 60% of the maximum reflectivity in unit dB); 2) apply a noise filter to remove small and isolated high reflectivity pixels; and 3) count the number of remaining reflectivity entities. The reflectivity map is classified as convective precipitation if multiple entities are found. Note that the entity test is not suited for differentiating blooms from stratiform rain where high reflectivity areas often appear as a large and continuous piece. In this case, a spectrum test is applied.

(*c) Spectrum Test*

While the entity features of blooms and stratiform rain are similar, the textures of two echo types are often different. Observations of large number of reflectivity images indicate that biological echoes, despite their continuous shape, appear to be loose and noisy, while stratiform precipitation echoes, appear to be solid and spatially coherent. AP echoes are usually noisy and lack of spatial coherency. Unfortunately, the local pixel-based texture properties of AP (e.g., 1st and 2nd order derivatives of reflectivity) can be very similar to those around convective storm cells. According to Chen et al. (2007), the power spectrum is particularly useful for isolating periodic structures or noise in 2-D images through some morphological analyses. Through Fourier transformation, a sharp discontinuity in the physical (spatial) domain will result in a peak in the frequency domain. Therefore, some texture differences between bloom/AP echoes and stratiform precipitation that are hard to identify in spatial domain may become distinguishable in the spectrum domain.

The Fourier Transform is an important image-processing tool that decomposes an image into a series of sinusoid functions and transforms a spatial image into a frequency (or “spectrum”) image. Each point in the spectrum image represents the magnitude of a particular sinusoidal frequency (or wavelength) contained in the original spatial image. For a square image of N×N pixels, the two-dimensional Discrete Fourier Transform (DFT) is given by:

$$F(u,v) = \sum_{x=0}^{N-1} \sum_{y=0}^{N-1} f(x,y) e^{-j2\pi\left(\frac{ux}{N}+\frac{vy}{N}\right)}$$

where $f(x,y)$ is the image in the spatial domain and the exponential term is the basis function corresponding to each point $F(u,v)$ in the frequency domain.

The power spectrum image is a plot of squared magnitudes of various frequency components in a 2-D frequency domain (Figs. 5d, 5e, and 5f). The 2-D frequency domain is centered at the origin and each axis represents the sinusoidal frequencies along the x and y directions in the spatial domain. To enhance the visibility of frequency components that are weakly visible on the power spectra plot, 1) firstly, the pixel values of the spatial image (the reflectivity echo map) are put as the exponents of a base of 1000 and then 2-D image matrix is normalized; 2) after DFT process, the power spectrum matrix is converted to logarithmic scale and then normalized. Fig.5 shows the power spectrum plots for a bloom, an AP, and a stratiform snow event. The snow event is characterized by a distinct, well-organized stripe pattern, while the bloom

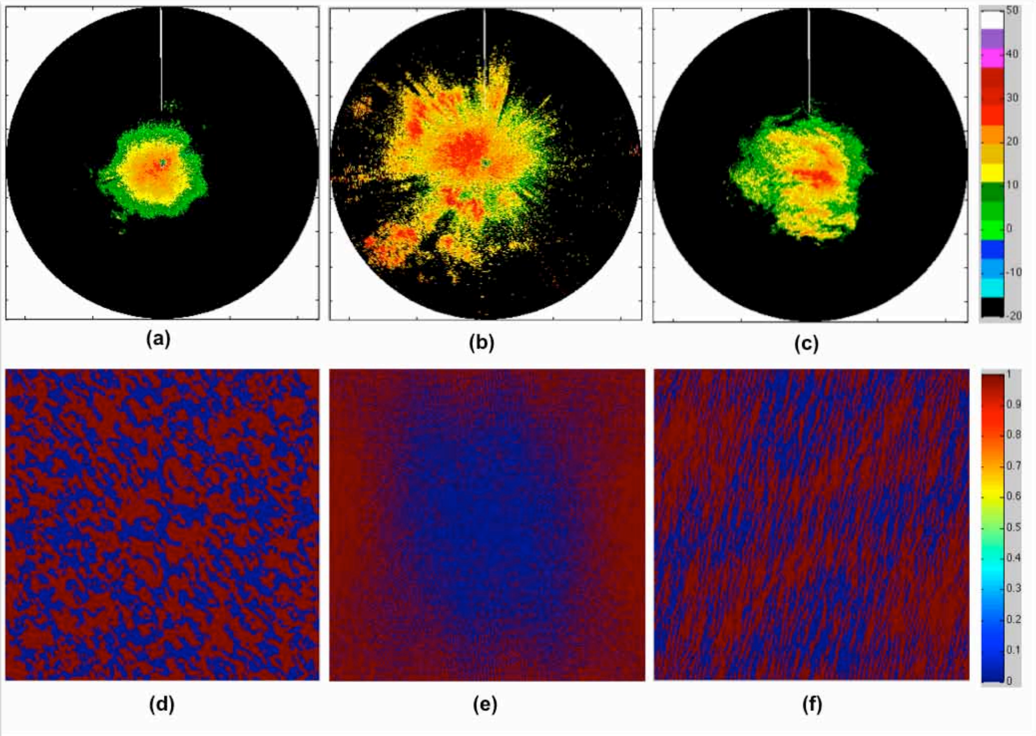

Figure 5. Base reflectivity maps and corresponding power spectrum plots for a bloom (a), an AP (b), and a striform rain (c). Data are collected from KDLH on May 4th, 2010 at 04:13 UTC (a); KLCH on May 10th, 2010 at 04:09 UTC (b); and KMVX on May 7th, 2010 at 04:07 UTC (c), respectively.

and AP events show unorganized patterns.

Morphological analyses are performed on the spectrum images for pattern recognition. Because a stripe pattern has significantly larger gradient variations in one direction than others, the accumulations of absolute values of the gradient between every adjacent pixel pair are calculated along eight pre-defined directions. After comparing the accumulated gradients among the eight directions, an image is classified as "stripe" type that is associated with precipitation echoes, when the ratio of the maximum over minimum gradient sums exceeds a given threshold.

It is noteworthy that the spectrum test cannot be used to separate blooms from convective rain echoes. Convective rainfalls usually have multiple and sparsely distributed echo blocks that would result in a spectrum image with little stripe properties.

(*d) Bloom/AP Censor Algorithm*

The three tests described in the previous sections are combined to form a four-step bloom/AP censor algorithm. The flowchart is demonstrated in Fig.6. Detailed descriptions of each step are provided below.

The global tilt test (I) is applied firstly with the input of a complete volume scan. Two polar-grid reflectivity maps are selected from the lowest two tilts that are at least 1-degree apart in elevation angles. Depending on the volume coverage patterns (VCP) associated with the data, the two tilts could be the 1st and 2nd (e.g., VCP 21 and 11) or the 1st and 4th (e.g., VCP12). If the reduction in the size of echoes from the 1st and the 2nd (or 4th) tilts exceeds a certain threshold, then the echoes on the 1st tilt are considered as pure (or being dominated by) bloom/AP and are completely removed. Otherwise, the reflectivity fields are unchanged and passed to step (II), the local tilt tests. After the separation of blooms from possible precipitation echoes located away from the radar site, the bloom echoes surrounding the radar can be identified by a local tilt test. This step is similar to step (I) except that the echo size-reduction check only applies in the potential bloom region near the radar.

Bloom echoes during the peak of birds migrating seasons can be very deep and can sometimes fail the tilt test. When blooms occur under anomalous propagation conditions, they show up at a higher elevation than their actual location, making the tilt tests in steps (I) and (II) less effective. These blooms are subject to further screenings in steps (III) and (IV). In step (III), the entity test, very low reflectivity returns were filtered, and the rest of the echoes are grouped and an entity analysis is performed via a scheme of connected component labeling (Umbaugh, 2005). Convective rainfalls can be clearly distinguished from potential bloom/AP clutter when the echo image has multiple entities. The last screening step is to differentiate the noisy clutter echoes from stratiform precipitation. After calculations of DFT and power spectrum, the pattern recognition technique is performed to identify smooth/noisy maps (clutter) from stripe patterns (precipitation). All threshold parameters in Fig.6 are selected conservatively to

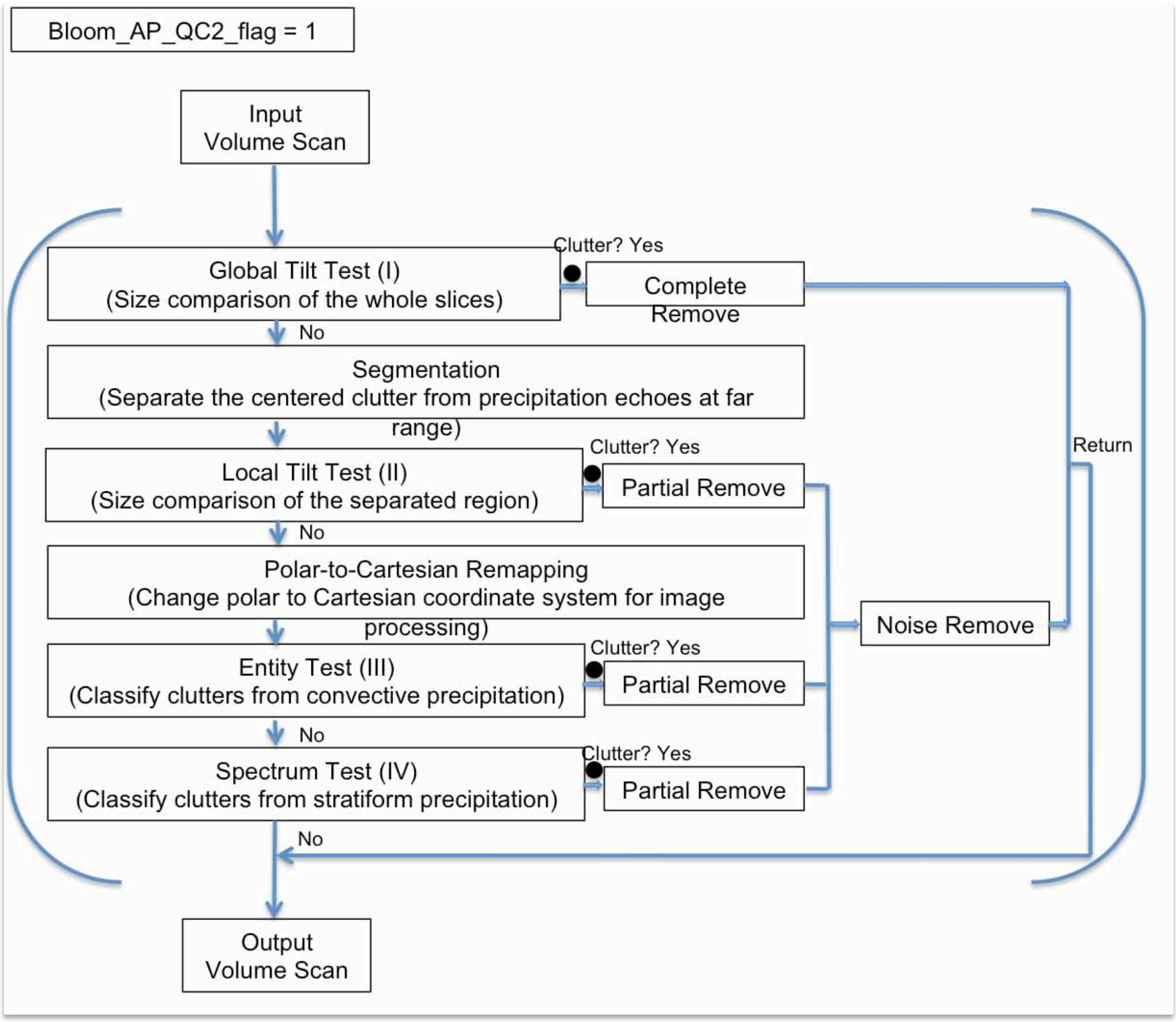

Figure 6. The flowchart of the Bloom/AP censor algorithm.

preserve precipitation echoes and to minimize false classifications of blooms/AP in precipitation areas. This is very important because the proposed algorithm is based on global echo properties and a false classification may lead to erroneous removal of true precipitation echoes on a large scale.

3. RESULTS AND DISCUSSIONS

The new bloom/AP identification algorithm was tested on more than 1600 volume scans of data observed from 59 radars among the United States Weather Surveillance Radar – 1988 Doppler (WSR-88D) network and 5 radars from the Chinese New Generation Weather Radar (CINRAD) network. The observations included blooms, AP, convective and/or stratiform precipitation, and bloom/precipitation mixture events. Over 90% of the blooms and AP echoes were effectively identified and removed, including cases where blooms and precipitation echoes co-existed within the same radar domain (but detached from each other). There was a very low false alarm rate (the rate of miss-identification of rainfall as blooms/AP) of 0.2% because of very conservative decisions for clutter removal (black dots in Fig. 6). The results demonstrated the good potential of using large-scale and physically based reflectivity properties and digital image processing techniques for segregation of precipitation and non-precipitation echoes. Specific examples are presented below.

Most of blooms that co-exist but not deeply mixed with precipitation echoes can be identified and removed in steps (II), (III) and (IV). Parameters in these steps are cautiously selected to keep light stratiform rainfall or snow echoes unmodified. Fig.7 shows an asymmetric bloom echo that co-exists with a stratiform precipitation but not mixed with the precipitation (Fig.7a). The bloom was successfully removed through the local tilt test (Fig.7b) after being segregated from the precipitation via the entity test. The precipitation, on the other hand was correctly retained.

When the 2-D reflectivity field is dominated by precipitation or when blooms/AP clutter are deeply mixed with precipitation echoes, the clutter cannot be segregated out by the proposed global processing technique. These reflectivity fields will be left unmodified and should be further processed using pixel-based reflectivity quality control techniques. Nevertheless, the current scheme can screen out a lots of bloom/AP data and reduce the computational cost for more sophisticated schemes downstream.

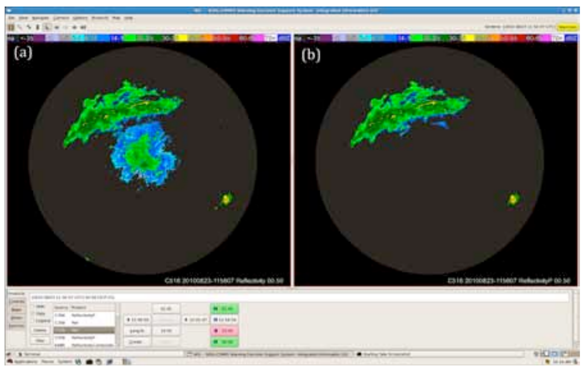

Figure 7. Base reflectivity on the 0.5° tilt before (a) and after (b) the bloom/AP QC when blooms are separated from precipitation echoes (data from China Radar C516 on August 23rd, 2010 at 11:56 UTC).

3. CONCLUSIONS

Biological scatterers and anomalous propagation often cause problems in weather radar applications in meteorology and in hydrology. In this work we attempt to address this issue from a global image processing aspect by treating each tilt of reflectivity fields as a 2-D digital image. Large-scale spatial properties of blooms/AP and precipitation echoes were analyzed, and a multi-step procedure was developed to identify blooms/AP echoes. The identification was based on entities instead of individual pixels. The new technique was tested on over 1600 volume scans of data from 60+ radars from different regions and seasons. The results showed that this technique is very effective in censoring blooms/AP echoes under clear air situations and when the blooms/AP echoes are separated from precipitation areas. It is computationally efficient and can be used as a pre-screening step for pixel-based reflectivity QC algorithms.

4. REFERENCES

Bachmann, S.M., and Tracy, M., 2009, DATA DRIVEN ADAPTIVE IDENTIFICATION AND SUPPRESSION OF GROUND CLUTTER FOR WEATHER RADAR, 25th Conference on International Interactive Information and Processing Systems (IIPS) for Meteorology, Oceanography, and Hydrology, Volume 11.B3: Phoenix, AZ.

Bäckmanf, J., and Alerstam, T., 2002, Orientation scatter of free-flying nocturnal passerine migrants: components and causes: Animal Behaviour, v. 65, p. 987-996.

Bøvith, T., Nielsen, A.A., Hansen, L.K., Overgaard, S., and Gill, R.S., 2006, Detecting Weather Radar Clutter by Information Fusion With Satellite Images and Numerical Weather Prediction Model Output, Proceedings of the IEEE Geoscience and Remote Sensing Symposium (IGARSS), p. 511-514.

CHO, Y.-H., LEE, G., KIM, K.-E., and ZAWADZKI, I., 2006, Identification and Removal of Ground Echoes and Anomalous Propagation Using the Characteristics of Radar Echoes: JOURNAL OF ATMOSPHERIC AND OCEANIC TECHNOLOGY, v. 23, p. 1206-1222.

FULTON, R.A., BREIDENBACH, J.P., SEO, D.-J., and MILLER, D.A., 1998, The WSR-88D Rainfall Algorithm: WEATHER AND FORECASTING, v. 13, p. 377-395.

GAUTHREAUX, S.A., and BELSER, C.G., 1998, Display of bird movements on the WSR-88D: Patterns and quantification: WEA THER AND FORECASTING, v. 13, p. 453-464.

Gray, W., and Larsen, H., 2004, RADAR RAINFALL ESTIMATION IN THE NEW ZEALAND CONTEXT., Sixth International Symposium on Hydrological Applications of Weather Radar: Melbourne, Australia.

HAMER, T.E., SCHUSTER, S.M., and MEEKINS, D., 2005, RADAR AS A TOOL FOR MONITORING XANTUS'S MURRELET POPULATIONS: Marine Ornithology, v. 33, p. 139-146.

Kessinger, C., Ellis, S., and Andel, J.V., 2003, The radar echo classifier: A fuzzy logic algorithm for the WSR-88D, 3rd Conference on Artificial Applications to the Environmental Science: Long Beach, CA, US.

Lakshmanan, V., and Zhang, J., 2009, Censoring Biological Echoes in Weather Radar Images, Sixth International Conference on Fuzzy Systems and Knowledge Discovery: Tianjin, China.

Lakshmanan, V., Zhang, J., and Howard, K., 2010, A Technique to Censor Biological Echoes in Radar

Reflectivity Data: Journal of Applied Meteorology, v. 49, p. 435-462.
LIU, S., XU, Q., and ZHANG, P., 2005, Identifying Doppler Velocity Contamination Caused by Migrating Birds. Part II: Bayes Identification and Probability Tests: JOURNAL OF ATMOSPHERIC AND OCEANIC TECHNOLOGY, v. 22, p. 1114-1121.
Martin, W.J., and Shapiro, A., 2007, Discrimination of Bird and Insect Radar Echoes in Clear Air Using High-Resolution Radars: JOURNAL OF ATMOSPHERIC AND OCEANIC TECHNOLOGY, v. 24, p. 1215-1230.
Michelson, D.B., and Sunhede, D., 2004, Spurious weather radar echo identification and removal using multisource temperature information: Meteorological Applications v. 11, p. 1-14.
Moszkowicz, S., Ciach, G.J., and Krajewski, W.F., 1994, Statistical Detection of Anomalous Propagation in Radar Reflectivity Patterns: JOURNAL OF ATMOSPHERIC AND OCEANIC TECHNOLOGY, v. 11, p. 1026-1034.
Pamment, J.A., and Conway, B.J., 1998, Objective Identification of Echoes Due to Anomalous Propagation in Weather Radar Data: JOURNAL OF ATMOSPHERIC AND OCEANIC TECHNOLOGY, v. 15, p. 98-113.
Schmaljohann, H., Liechti, F., and Bruderer, B., 2007, Songbird migration across the Sahara: the non-stop hypothesis rejected!: Proceedings of the Royal Society B, v. 274, p. 735-739.
STEINER, M., and SMITH, J.A., 2002, Use of Three-Dimensional Reflectivity Structure for Automated Detection and Removal of Nonprecipitating Echoes in Radar Data: JOURNAL OF ATMOSPHERIC AND OCEANIC TECHNOLOGY, v. 19, p. 673-686.
ZHANG, P., LIU, S., and XU, Q., 2005, Identifying Doppler Velocity Contamination Caused by Migrating Birds. Part I: Feature Extraction and Quantification: JOURNAL OF ATMOSPHERIC AND OCEANIC TECHNOLOGY, v. 22, p. 1105-1113.